Impact of Microstructure and Current Crowding on Electromigration: A TCAD Study

H. Ceric and M. Rovitto
Christian Doppler Laboratory for Reliability Issues in Microelectronics at the Institute for Microelectronics
Institute for Microelectronics, TU Wien, Gußhausstraße 27-29, 1040 Wien, Austria
Email: {ceric|rovitto}@iue.tuwien.ac.at

***Abstract*—Electromigration (EM) degradation and failure in modern interconnect structures are result of several physical phenomena acting together. In order to increase reliability thoroughly understanding of these phenomena and their interplay is necessary. In the case of dual-damascene technology both geometry and microstructure of the interconnect play an important role, determining the development of EM degradation. In this paper we use a state-of-the-art EM modeling and simulation for a comparative study of EM performance of standard straight interconnect structure and a structure with a right angle. It has been shown that by applying a detailed model of EM driven vacancy dynamics in the presence of grain boundaries, current crowding due to right angle of the interconnect geometry has a less impact than microstructure.**

I. Introduction

EM is one of the main reliability issues of Back End of Line (BEOL) which can trigger system failure at some undefined future time. The main challenge in EM modeling and simulation is the diversity of the relevant physical phenomena. Extensive EM experiments have produced an ample amount of data, indicating that the copper interconnect lifetime has decreased for every new interconnect generation, even when tested at the same current density. Newer interconnects, due to their reduced size, require a smaller void volume for failure and a larger fraction of atoms is transferred, along the fast interface, to the capping layer and the grain boundary diffusion paths.

The electromigration lifetime, depending on the variability of material properties at the microscopic and atomistic level, has always distributed values [1], [2]. Under microscopic properties we understand grain boundaries (GBs) and grains with their proper crystal orientation and under atomistic properties specific configuration of atoms inside the GBs, inside the interfaces to surrounding layers, and cross-section between GBs and interfaces. The dimensions of modern interconnect are in a region, where microscopic and atomistic properties are gaining importance. Therefore, in order to understand the distribution of EM lifetime, the variability of the impact parameters and their influence on EM must be well understood and appropriately modeled [3].

II. Electromigration Modeling

EM failure develops under the influence of different material, microstructural, and geometrical features. Different types of failure can be contributed to each of these impact factors or their combination. An impact of geometry can be observed in the case of dual-damascene interconnect structure where the liner separates two copper regions and interrupts material transport. This configuration leads to material depletion and void formation. The microstructure of interconnect metal has a significant impact on EM, because it introduces diversity of possible EM paths and local mechanical properties (the Young modulus and Poisson factor depend on the crystal orientation in each grain).

Comprehensive EM model includes beside EM itself as a main driving force, additional driving forces of vacancy concentration gradient, mechanical stress gradient, and temperature gradient. In the case study discussed in this work, temperature gradient may be neglected due to small dimensions and high thermal conductivity of copper. Components of the comprehensive EM model have evolved during several decades of development [4], [5], [6], [7], [8], [9]. Components of the state-of-the-art EM model, introduced in [10], which have been utilized in the present study are presented in the follwoing sections.

A. Driving Forces

Material transport is driven by the EM ($\sim \nabla\varphi$), by the vacancy concentration gradient ($\sim \nabla C_v$), and by the stress gradient ($\sim \nabla \mathrm{tr}(\bar{\bar{\sigma}})$) [9],

$$\vec{J}_v = \mathbf{D}^v \Big(\frac{Z^* e}{k_B T} C_v \nabla\varphi + \nabla C_v + \frac{f\Omega}{3\, k_B T} C_v \nabla \mathrm{tr}(\bar{\bar{\sigma}}) \Big), \quad (1)$$

$$\frac{\partial C_v}{\partial t} = -\nabla \cdot \vec{J}_v + G(C_v). \quad (2)$$

$\mathbf{D}^v$ is the tensorial vacancy diffusivity, which is in a stress free state and set as $D^v_{ij} = D_{bulk}\delta_{ij}$, where D_{bulk} is the isotropic bulk diffusivity. $G(C_v)$ is the vacancy recombination/annihilation source term related to GBs' physics.

B. Anisotropic Diffusivity

The local stress state introduces an anisotropy of the diffusivity. The dependence of the tensorial diffusivity on the stress state is given by the following relationship [11]:

$$D^v_{ij} = \frac{\Gamma_0}{2} \sum_{k=1}^{12} x^k_i x^k_j \exp\Big(-\frac{\bar{\varepsilon}^k_I \Omega\, (\mathbf{C}\bar{\varepsilon})}{k_B T} \Big) \quad (3)$$

x^k_i is the i^{th} component of the jump vector $\vec{r}^k$ for a site k, $\bar{\varepsilon}$ is the acting anisotropic strain, $\mathbf{C}$ is the elasticity tensor, $\bar{\varepsilon}^k_I$ is the strain induced by a single vacancy in the jump direction defined by the unit vector $\vec{n}_k = \vec{r}^k/|\vec{r}^k|$, and Γ_0 is the vacancy-atom exchange rate. The basis for this model was first presented in the theory of Dederichs *et al.* [12].

978-1-4673-7860-4/15/$31.00 ©2015 IEEE

C. Microstructure

It is well known today that the microstructure of copper has a significant impact on electromigration failure. GBs are fast diffusivity paths and vacancy recombination sites [13]. The diffusion of vacancies in the grain boundary is faster compared to diffusion in the grain bulk, because a grain boundary generally exhibits a larger diversity of point defect migration mechanisms. Formation energies and migration barriers of point defects are in average lower than those for lattice [14].

Different modeling approaches [9], [13], [15] have been utilized aiming to describe all physical mechanisms present in GBs. The approach applied in this work is comprised in the expression for vacancy anihilation/recombination term

$$G(C_v) = -\frac{1}{\tau}\Big(C_v^{eq} - C_v^{im}\Big(1 + \frac{2\,\omega_R}{\omega_T(C_{v,1}+C_{v,2})}\Big)\Big), \quad (4)$$

where

$$\frac{1}{\tau} = \frac{\omega_T(C_{v1}+C_{v2})}{\delta_{gb}}, \quad (5)$$

and C_{v1} and C_{v2} are vacancy concentration from both sides of GB, C_v^{im} is the concentration of vacancy inside the GB, and ω_R and ω_T are the vacancy release and trapping rate, respectively. δ_{gb} is the GB thickness. The derivation of the above GB model which is based on a segregation model [16] is discussed in [9].

D. Mechanical Stress

Divergences of the vacancy flux produce local strain [7]

$$\frac{\partial \varepsilon_{ij}^v}{\partial t} = \frac{1}{3}\Omega\big[(f\nabla\cdot\vec{J}_v + (1-f)G(C_v)\big]\delta_{ij}. \quad (6)$$

In order to obtain a complete picture of stress tensor in the all the points of the geometry, considering all necessary boundary conditions, equilibrium equations need to be solved

$$\mu\nabla^2 u_i + (\lambda+\mu)\frac{\partial}{\partial x_i}(\nabla\cdot\vec{u}) = B\frac{\partial}{\partial x_i}\mathrm{tr}(\bar{\bar{\varepsilon}}^v), \quad i=1,2,3 \quad (7)$$

where λ and μ are the Lame coefficients, $B = \lambda + 2\mu/3$, and $\mathbf{u} = (u_1, u_2, u_3)$ is the displacement vector which is connected to the strain tensor $\bar{\bar{\varepsilon}}$ and the stress tensor with relationships

$$\varepsilon_{ij} = \frac{1}{2}\Big(\frac{\partial u_i}{\partial x_j} + \frac{\partial u_j}{\partial x_i}\Big), \quad (8)$$

$$\sigma_{ij} = \lambda\mathrm{tr}(\bar{\bar{\varepsilon}})\delta_{ij} + 2\mu\varepsilon_{ij}. \quad (9)$$

E. Voiding

Equations (1)-(9) can be solved by a general finite element method (FEM) simulation tool for arbitrary three dimensional interconnect geometry. As a solution we obtain $C_v(x,y,z)$ and $\bar{\bar{\sigma}}(x,y,z)$ in all the points of the studied geometry. The rapid phase of the EM degradation starts with a void nucleation, which is initiated when stress threshold σ_{th} is attained at some point of the interconnect geometry. According to [17], [18] the stress threshold σ_{th} is determined as

$$\sigma_{th} = \frac{2\gamma_s \sin\theta_c}{R_p}. \quad (10)$$

Usually voids nucleate at the small patch of weak adhesion which is characterized by a radius R_p and contact angle θ_c as

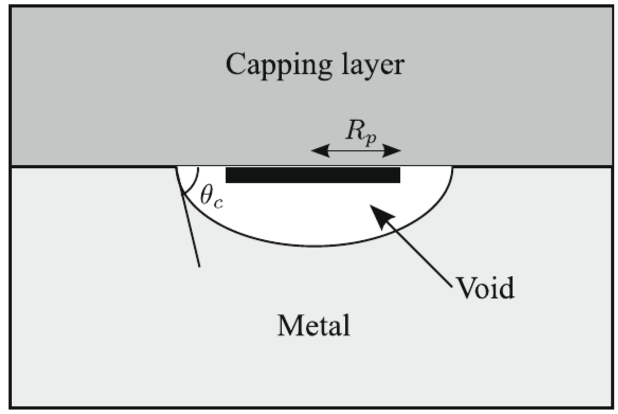

Fig. 1. Schematic void nucleation at an interface site of weak adhesion.

shown in Fig. 1. A combination of theoretical and experimental investigation have shown that a natural sites of weak adhesion are the “triple-points” - sites where copper GBs meet interfaces [9].

F. Electric Field Singularities

Right angles in the interconnect structures are sites where current density gets very high. The exact solution of the Laplace equation produces for these sites a singularity in the current density. The approximate solution obtained by the FEM analysis with linear or square shape functions cannot produce singularities but high finite values of the current density. The finer we choose the simulation mesh (c.f. Fig. 2) in the vicinity of the edge, the exact solution is better approximated in this area and the higher is also the calculated peak value of the current density [19]. If r is the distance from the angle point, the peak current density is given by [20], [19]

$$|\vec{J}| \sim \gamma\frac{1}{r^{1/3}}, \quad (11)$$

where γ is the electric conductivity.

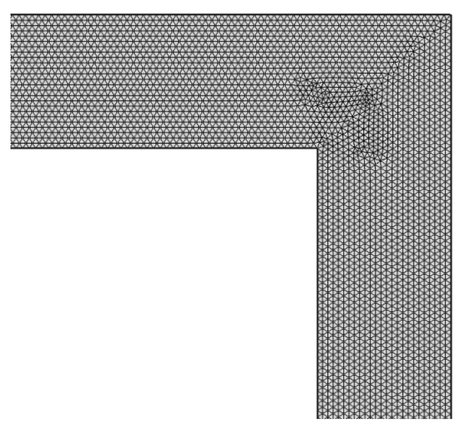

Fig. 2. Dense FEM mesh at the interconnect angle needed to ensure accuracy of calculation.

Interconnect technology can never produce a perfect, sharp right angles. However even if we define an angle with a small

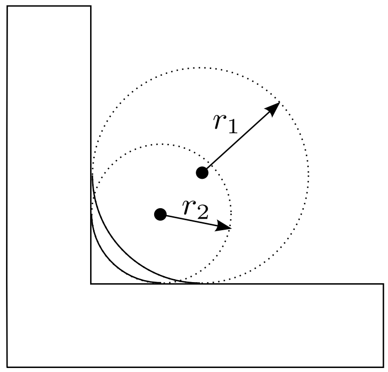

Fig. 3. Characterization of angle sharpness.

circular fillet arc (c.f. Fig. 3) the peak current density increases very fast with a smaller arc radius r as presented in Fig. 4.

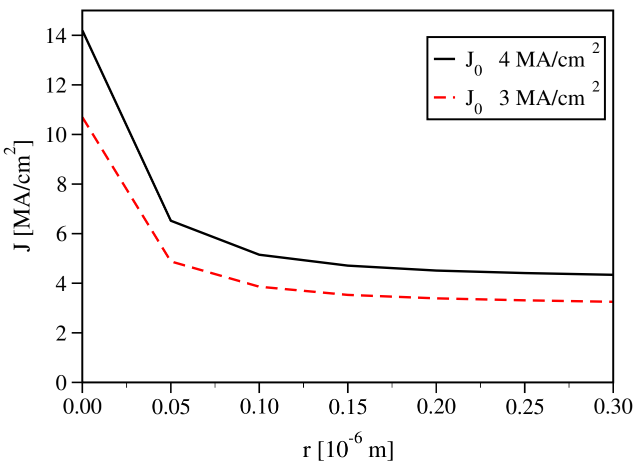

Fig. 4. Increase of a peak current density with a smaller arc radius r.

Since EM driven vacancy flux is according to (1)

$$|\vec{J}_v| \sim \frac{Z^* e}{k_B T} C_v |\vec{J}| \tag{12}$$

it is plausible to expect that in the presence of right angles in the interconnect EM degradation is significantly intensified.

III. Simulative Study

A. Experimental Observations

An interesting example of an influence of different factors on EM failure is provided in the experimental study Croes *et al.* [21]. In this study, the development of EM failure has been studied in both straight and angled interconnects under the same testing conditions. It was natural to expect that the current crowding produced in the right angle interconnect corner would intensify EM and lead to a shorter lifetime of the studied interconnect structure.

However, in the lognormal probability plots of the failure times obtained on both the standard straight and angled structure for the three different line widths no difference in failure times is observed [21]. This indicates that the current crowding and current density gradient induced in the angled structure have no effect on EM lifetimes, also not in the lower percentile.

Determination of void location was done using top-down SEM after removing the top passivation layers. No voiding has been observed directly in the interconnect corner, voids seem to appear randomly along the interconnect line [21].

B. Analysis

Experimentally observed behavior implies that while both microstructural and geometric factors play important roles, microstructure, e.g., distribution of GBs has the more significant impact. Sites where GBs meet liner or etch stop interface, are, as previous studies have shown [9], natural points of weak adhesion where, given high tensile stress and vacancy concentration, voids nucleate. Growth and movement of void inside interconnect line finally lead to resistance increase and failure. We have applied the full physical EM model [10] including (1)-(9) to study failure development in these geometries.

The model has been implemented in COMSOL MULTIPHYSICS [22] simulation tool. In Fig. 5 the geometries utilized in this study are presented. In both interconnects GBss are indicated. For assumed interconnect width of 80nm GBss are distributed in the near bamboo manner as it could be expected for these dimensions and applied technology. As we have seen in Section II-F close to the interconnect corner we have a high current density and according to (12) an intensive material transport have to be expected. However, even in this particular conditions, EM simulations produce a typical three-phase growth of vacancy concentration [5]. Peak vacancy concentration and corresponding peaks of tensile stress develop at the geometrical ends of studied interconnect shapes and at the triple-points of microstructure. In the studied case, naturally, the triple points stress peaks are more important, particularly those which are distributed in the vicinity of current crowding region. In Fig. 6 and Fig. 7 vacancy concentration and tensile

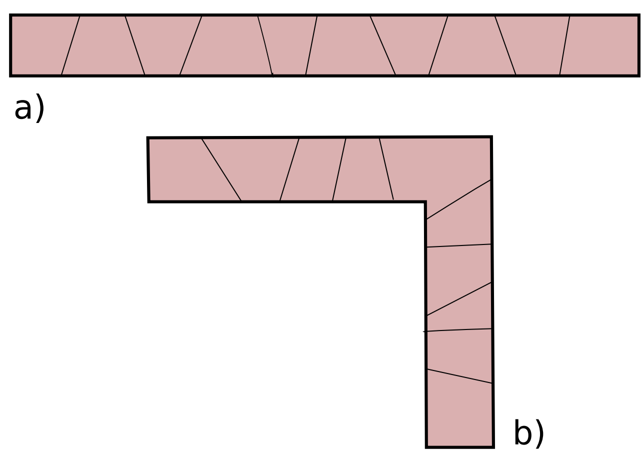

Fig. 5. a) Linear and b) L-shaped geometry used in the study.

stress dynamics are presented, respectively. As we can see in these figures the differences between vacancy concentration and stress dynamics in the linear and angled interconnects are quite small.

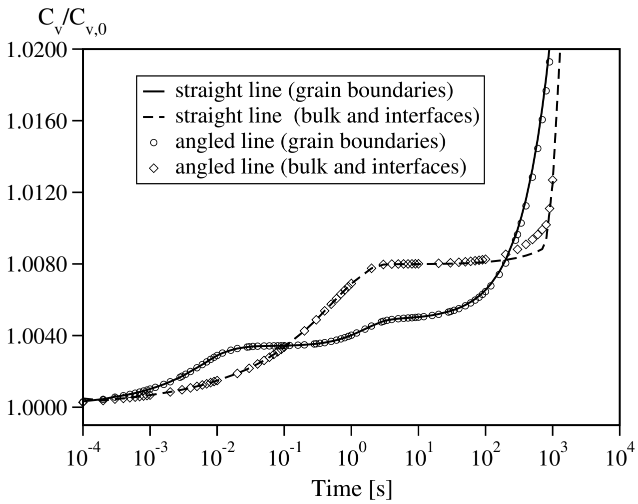

Fig. 6. Growth of peak vacancy concentration induced by EM at the microstructure triple-points for linear and L-shaped geometry.

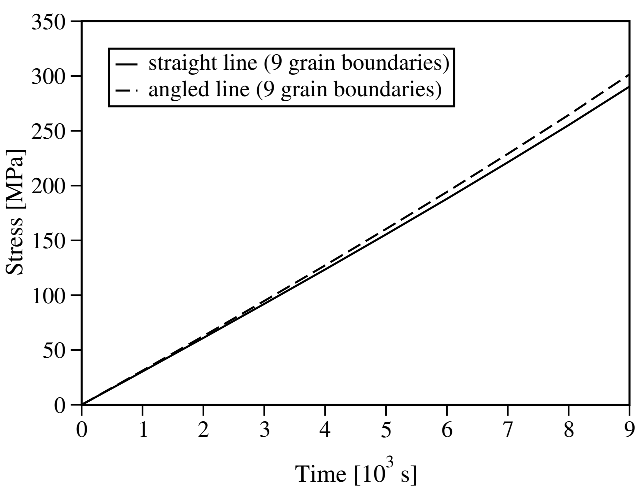

Fig. 7. Growth of peak tensile stress induced by EM at the microstructure triple-points for linear and L-shaped geometry.

IV. Conclusion

In the presented work an analysis of EM failure in two different interconnect geometries has been carried out. The first geometry was a straight interconnect and the second angled (L-shaped) interconnect. Angled interconnect produces a high current density and correspondingly an intensive material transport induced by EM. Using the state-of-the-art EM modeling both interconnect structures have been analyzed and the results have been compared with the original experimental observations. Simulation produced peak vacancy concentration and mechanical stress dynamics which show no difference for the two simulated interconnect geometries. EM voiding is not determined by a presence of electric field singularity at the interconnect corner but by the distribution of GBs, i.e. triple points. The conclusion is that the current crowding in the given situation has a less significant impact on the failure development than GBs distribution.

References

[1] J. Lloyd and K. P. Rodbell, "Reliability," *in Handbook of Semiconductor Interconnection Technoogy, edited by G.C. Schwartz and K. V. Srikrishnan*, pp. 471–520, 2006.

[2] C. M. Tan and A. Roy, "Electromigration in ULSI Interconnects," *Mat. Sci. Eng.*, vol. 58, no. 1-2, pp. 1–75, 2007.

[3] C. Ryu, K.-W. Kwon, A. L. S. Loke, H. Lee, T. Nogami, V. M. Dubin, R. A. Kavari, G. W. Ray, and S. Wong, "Microstructure and Reliability of Copper Interconnects," *IEEE Trans. Elec. Dev.*, vol. 46, pp. 1113–1120, 6.

[4] M. Shatzkes and J. R. Lloyd, "A Model for Conductor Failure Considering Diffusion Concurrently with Electromigration Resulting in a Current Exponent of 2," *J. Appl. Phys*, vol. 59, no. 11, pp. 3890–3893, 1986.

[5] R. Kirchheim and U. Kaeber, "Atomistic and Computer Modeling of Metallization Failure of Integrated Circuits by Electromigration," *J. Appl. Phys.*, vol. 70, no. 1, pp. 172–181, 1991.

[6] M. A. Korhonen, P. Borgesen, K. N. Tu, and C. Y. Li, "Stress Evolution Due to Electromigration in Confined Metal Lines," *J. Appl. Phys.*, vol. 73, no. 8, pp. 3790–3799, 1993.

[7] M. E. Sarychev and Y. V. Zhitnikov, "General Model for Mechanical Stress Evolution During Electromigration," *J. Appl. Phys.*, vol. 86, no. 6, pp. 3068 – 3075, 1999.

[8] V. Sukharev, A. Kteyan, E. Zschech, and W. D. Nix, "Microstructure Effect on EM-Induced Degradations in Dual Inlaid Copper Interconnects," *IEEE Trans. Dev. Mat. Rel.*, vol. 9, no. 1, pp. 87–97, 2009.

[9] H. Ceric, R. L. de Orio, J. Cervenka, and S. Selberherr, "A Comprehensive TCAD Approach for Assessing Electromigration Reliability of Modern Interconnects," *IEEE Trans. Dev. Mat.Rel.*, vol. 9, no. 1, pp. 9–19, 2009.

[10] R. L. de Orio, "Electromigration Modeling and Simulation," Dissertation, Technische Universität Wien, 2010.

[11] R. L. de Orio, H. Ceric, and S. Selberherr, "Effect of Strains on Electromigration Material Transport in Copper Interconnect Structures under Electromigration Stress," *J. Comput. Electron.*, vol. 7, no. 3, pp. 128–131, 2008.

[12] P. H. Dederichs and K. Schroeder, "Anisotropic Diffusion in Stress Fields," *Phys. Rev. B*, vol. 17, no. 6, pp. 2524–2536, 1978.

[13] R. Rosenberg and M. Ohring, "Void Formation and Growth During Electromigration in Thin Films," *J. Appl. Phys.*, vol. 42, no. 13, pp. 5671–5679, 1971.

[14] M. R. Sorensen, Y. Mishin, and A. F. Voter, "Diffusion Mechanisms in Cu Grain Boundaries," *Phys. Rev. B*, vol. 62, no. 6, pp. 3658–3673, 2000.

[15] J. C. Fisher, "Calculation of Diffusion Penetration Curves for Surface and Grain Boundary Diffusion," *J. Appl. Phys.*, vol. 22, no. 1, pp. 74–77, 1951.

[16] F. Lau, L. Mader, C. Mazure, C. Werner, and M. Orlowski, "A Model for Phosporus Segregation at the Silicon - Silicon Dioxide Interface," *Appl. Phys. A*, vol. 49, pp. 671–675, 1989.

[17] B. M. Clemens, W. D. Nix, and R. J. Gleixner, "Void Nucleation on a Contaminated Patch," *J. of Materials Research*, vol. 12, no. 8, pp. 2038–2042, 1997.

[18] R. J. Gleixner, B. M. Clemens, and W. D. Nix, "Void Nucleation in Passivated Interconnect Lines: Effects of Site Geometries, Interfaces, and Interface Flaws," *J. of Materials Research*, vol. 12, pp. 2081–2090, 1997.

[19] R. Sabelka, "Dreidimensionale Finite Elemente Simulation von Verdrahtungsstrukturen auf Integrierten Schaltungen," Dissertation, Technische Universität Wien, 2001.

[20] J. D. Jackson, *Classical Electrodynamics*. John Wiley and Sons, Inc., 1999.

[21] K. Croes, Y. Li, M. Lofrano, C. J. Wilson, and Z. Tokei, "Intrinsic Study of Current Crowding and Current Density Gradient Effects on Electromigration in BEOL copper interconnects," *Proc. Intl. Reliab. Phys. Symp.*, pp. 2C.3.1–2C3.4, 2013.

[22] *COMSOL, Inc., Burlington, MA. 8 New England Executive Park.*